Antioscillatory Effects of Nociceptin/Orphanin FQ in Synaptic Networks of the Rat Thalamus

Susanne Meis, Thomas Munsch, and Hans-Christian Pape

Institut für Physiologie, Otto-von-Guericke-Universität, D-39120 Magdeburg, Germany

Postsynaptic and presynaptic effects of nociceptin/orphanin FQ (N/OFQ), the endogenous ligand of the opioid-like orphan receptor, were investigated in an *in vitro* slice preparation of the rat thalamic reticular nucleus (NRT) and ventrobasal complex (VB). In NRT as well as VB, all tested neurons developed an outward current on application of 1 μM N/OFQ. Basic properties of the N/OFQ-induced current included inward rectification, dependence on extracellular K^+, reduction by 100 μM Ba^+, antagonistic effect of [Nphe^1]nociceptin(1–13)NH_2, and sensitivity to internal GDP-β-*S*. Miniature IPSCs (mIPSCs) mediated by $GABA_A$ receptors in VB neurons were not affected by 1 μM N/OFQ. In addition, paired-pulse depression of evoked IPSCs was unchanged, indicating a lack of presynaptic effects. By comparison, N/OFQ application resulted in a reduction in frequency of miniature EPSCs (mEPSCs) in a subpopulation of NRT neurons, whereas paired-pulse facilitation of evoked EPSCs was not altered. In either nucleus, current-clamp experiments revealed a hyperpolarization and associated decrease in input resistance in response to N/OFQ. Although N/OFQ had no measurable effect on calcium-mediated burst activity evoked by depolarizing steps from hyperpolarized values of the membrane potential, rebound bursts on relief of hyperpolarizing current steps were decreased. Slow thalamic oscillations induced *in vitro* by extracellular stimulation were dampened by N/OFQ in VB and NRT, as seen by delayed onset of rhythmic multiple-unit activity and reduction in amplitude and duration. We conclude that N/OFQ reduces the excitability of NRT and VB neurons predominantly through an increase of a G-protein-coupled inwardly rectifying K^+ conductance.

Key words: thalamus; electrophysiology; patch-clamp; neuropeptide; potassium inward rectifier; synaptic transmission

A peptide termed nociceptin/orphanin FQ (N/OFQ) was recently identified as an endogenous heptadecapeptide agonist for the opioid receptor-like (ORL) receptor. Despite many structural homologies to opioid receptors, the ORL receptor shows low-affinity binding to selective opioid agonists or antagonists. N/OFQ selectively activates the ORL receptor but not any opioid receptor subtype (Calo' et al., 2000b). In contrast to behavioral effects of classical opioids, N/OFQ was originally described as pronociceptive (Meunier et al., 1995; Reinscheid et al., 1995). In close succession, N/OFQ was shown to elicit a wide range of behavioral responses in view of pain processing, including hyperalgesia, reversal of opioid-mediated analgesia, analgesia, and allodynia, and was described as "opiate modulating" (for review, see Yamamoto et al., 1999; Barlocco et al., 2000; Brundege, 2000; Grisel and Mogil, 2000; Harrison and Grandy, 2000; Xu et al., 2000). On the cellular level, effects of N/OFQ resemble those elicited by opioids (Standifer and Pasternak, 1997), including inhibition of cAMP formation, modulation of Ca^{2+} and K^+ conductances, and regulation of transmitter release (Calo' et al., 2000b; Hawes et al., 2000; Moran et al., 2000; Schlicker and Morari, 2000).

The thalamus is considered to be a crucial relay for the reception and processing of nociceptive information en route to the cortex (Millan, 1999). Opioids were demonstrated to modulate thalamic nociceptive cell activity (Shigenaga and Inoki, 1976; Benoist et al., 1986). Furthermore, neurons throughout the entire thalamus were reportedly inhibited by μ-opioid peptides through activation of an inwardly rectifying potassium conductance (Brunton and Charpak, 1997, 1998).

In the thalamus, peptide and precursor protein preproN/OFQ mRNA are expressed in a nucleus-specific manner, with high levels occurring in the thalamic reticular nucleus (NRT) (Ikeda et al., 1998; Neal et al., 1999b). Low to moderate signals for the ORL receptor were found throughout thalamic nuclei as was confirmed by *in vitro* receptor autoradiography, ligand-stimulated *in situ* [^{35}S]GTP-γ-*S* binding, and *in situ* hybridization (Shimohira et al., 1997; Sim and Childers, 1997; Ikeda et al., 1998; Neal et al., 1999a; Letchworth et al., 2000).

These results prompted us to analyze the role of N/OFQ in thalamic neurons in terms of presynaptic and postsynaptic actions using electrophysiological techniques in the rat thalamus *in vitro*. The intrinsic membrane properties in conjunction with the synaptic interplay between NRT and adjacent thalamic relay neurons support the generation of rhythmic activities characteristic of thalamic function (Steriade et al., 1997), which can be maintained *in vitro* (Huguenard and Prince, 1994). In the present study, attention therefore was focused on properties of NRT neurons and neurons out of the ventrobasal complex (VB).

MATERIALS AND METHODS

Slice preparation. Slices were prepared as described previously (Meis and Pape, 2001). Briefly, male or female Long–Evans rats (postnatal days 12–18) were decapitated after deep anesthesia with halothane. Part of the brain including the thalamus was removed and transferred into ice-cold oxygenated solution of the following composition (in mM): KCl 2.4, $MgSO_4$ 10, $CaCl_2$ 0.5, PIPES 20, glucose 10, sucrose 195, pH 7.35.

Received July 12, 2001; revised Nov. 20, 2001; accepted Nov. 21, 2001.

This work was supported by the Leibniz-Programm of the Deutsche Forschungsgemeinschaft (H.-C.P.), and by the Kultusministerium des Landes Sachsen-Anhalt. We thank R. Ziegler for expert technical assistance.

Correspondence should be addressed to Susanne Meis, Institut für Physiologie, Medizinische Fakultät, Otto-von-Guericke-Universität, Leipziger Strasse 44, D-39120 Magdeburg, Germany. E-mail: susanne.meis@medizin.uni-magdeburg.de.

 0270-6474/02/220718-10$15.00/0

Horizontal slices (300 μm thick) were cut using a Vibratome (Model 1000; Technical Products Inc., St. Louis, MO) and incubated in standard ACFS containing (in mM): NaCl 120, KCl 2.5, NaH_2PO_4 1.25, $NaHCO_3$ 22, $MgSO_4$ 2, $CaCl_2$ 2, glucose 10, bubbled with 95% O_2/5% CO_2 to a final pH of 7.3. Single slices were then placed in a submersion chamber, fixed by a silk mesh, and perfused continuously at a rate of ~2 ml/min at room temperature (24–25°C) with ACSF.

Recording techniques. The whole-cell patch-clamp technique was applied on NRT or VB neurons by a patch-clamp amplifier (EPC-7, List Medical Systems, Darmstadt, Germany). Recordings were made under visual control by use of infrared videomicroscopy (Axioskop FS, Achroplan 40/w; Zeiss, Oberkochen Germany; Imago camera, T.I.L.L. Photonics, Martinsried, Germany). Patch pipettes were pulled from borosilicate glass (GC150TF-10, Clark Electromedical Instruments, Pangbourne, UK) to resistances of 2–2.5 MΩ. Access resistance amounted to ~5 MΩ. Errors attributable to series resistance were <5 mV. A liquid junction potential of 10 mV of the standard pipette solution was corrected for (Neher, 1992). This solution contained (in mM): Kgluconate 95, K_3citrate 20, NaCl 10, HEPES 10, $MgCl_2$ 1, $CaCl_2$ 0.1, KBAPTA 1, MgATP 3, pH 7.2 with KOH. In some experiments, 2 mM GDP-β-*S* was included. Evoked IPSCs and spontaneous IPSCs (mIPSCs) were recorded with a pipette solution composed of (in mM): Csgluconate 117, CsCl 13, Nagluconate 5, Kgluconate 5, HEPES 10, $MgCl_2$ 1, $CaCl_2$ 0.1, EGTA 1.1, MgATP 3, pH 7.2 with KOH. For current-clamp recordings, pipettes were filled with (in mM): Kgluconate 120, HEPES 10, EGTA 5, $MgCl_2$ 2, $CaCl_2$ 0.5, KCl 2.5, MgATP 3, pH 7.2 with KOH. For characterizing the reversal potential of the N/OFQ-induced current, the extracellular KCl concentration was elevated to 5, 7.5, or 10 mM by substitution of an equimolar amount of NaCl. mIPSCs were recorded in ACSF likewise modified (5 mM KCl). Spontaneous postsynaptic currents were isolated in the presence of 1 μM tetrodotoxin (TTX). Records were low-pass filtered at 2.5 kHz (eight-pole Bessel filter). After the whole-cell configuration was obtained, neurons were held routinely at −70 mV or at 0 mV for IPSCs and mIPSCs, respectively, unless indicated otherwise. A bipolar tungsten electrode (Science Products, Hofheim, Germany; WPI, Sarasota, FL) was placed parallel to the borderline of the NRT within the VB for evoking IPSCs in VB neurons or parallel to the borderline of the VB within the NRT for evoking EPSCs in NRT neurons, respectively. IPSCs and EPSCs were elicited by two consecutive stimuli of 100 μsec duration delivered by a stimulus isolator (Isoflex, AMPI, Jerusalem, Israel), separated by an interstimulus interval of 100 or 50 msec, respectively. Stimulus amplitude was adjusted to evoke synaptic responses ~50% of the maximal amplitude without triggering multipeaked PSCs.

Extracellular multiple-unit activities were recorded with tungsten microelectrodes (50 MΩ, WPI) and an AC-coupled amplifier (DAM 80, WPI) using a bandwidth of 30 Hz-3 kHz. Extracellular $MgSO_4$ was replaced by 0.8 mM $MgCl_2$. Stimuli of 1 msec duration were delivered every 30 sec through a bipolar tungsten electrode placed into the internal capsule.

Drugs were added to the external ACFS. All substances were obtained from Sigma (Diesenhofen, Germany), except for N/OFQ (Gramsch Laboratories, München, Germany), NBQX (Tocris, Langford, UK), and [Nphe^1]nociceptin(1–13)NH_2 (Neosystem, Strasbourg, France).

Data analysis. Patch-clamp recordings and data analysis were performed using pClamp software version 6.0 operating via a Digidata 1200 interface board (Axon Instruments, Foster City, CA). Miniature postsynaptic currents were detected by the program "Mini-Analysis" (Jaejin software, Leonia, NJ). Cumulative histograms without bins were calculated within time periods of equal duration (1–3 min) before and after addition of N/OFQ. The peak current amplitudes of PSCs were derived from averages of three to four consecutive responses elicited at 0.05–0.067 Hz and were normalized with respect to the average value of the responses within a period of 12 min before addition of the drug. For determining changes in paired-pulse depression or facilitation, second IPSC/EPSC amplitudes were normalized according to first IPSC/EPSC amplitudes.

Extracellular multiple-unit activities were recorded and analyzed using spike 2 software operating through a CED 1401 interface (Cambridge Electronic Design, Cambridge, UK). Poststimulus time histograms were constructed averaging eight consecutive responses over a period of 6 sec with a bin size of 10 msec. Autocorrelograms were calculated from the average of three responses over a period of 5–6 msec with a bin size of 5 msec. Activity above 5% of first peak amplitude was used for calculation of cycle duration.

Statistical analysis was performed using Origin software (Microcal Northampton; Student's *t* test, Student's paired *t* test) or Mini-Analysis (Jaejin software; Kolmogorov–Smirnov two-sample test). Data are presented as mean ± SEM, before (control) and during maximal responses to the drug. Because recovery from responses to N/OFQ could not be obtained, N/OFQ was applied only once to each slice.

RESULTS

Properties of the N/OFQ-induced current in NRT neurons

In the NRT, the application of N/OFQ induced an outward current in all tested neurons at a holding potential of −70 mV ($n = 57$). The outward current commenced ~30 sec after addition of the drug and amounted to 47.6 ± 3.4 pA at 1 μM N/OFQ ($n = 14$) (Fig. 1*A*). The associated increase in membrane conductance was revealed by imposing hyperpolarizing voltage steps of 350 msec duration applied between −80 and −140 mV in 10 mV increments, as shown on an expanded time scale in Figure 1*B*. Subtracting currents before and after addition of N/OFQ yielded a difference current with rapid activation and no inactivation during 350 msec. Ramp-pulse voltage commands (0.2 mV/msec) repeatedly applied at 0.07 Hz from −70 to −140 mV were used to monitor the current–voltage (*I–V*) relationship (Fig. 1*C*). The current induced by N/OFQ showed moderate inward rectification and reversed at −97.0 ± 1.0 mV ($n = 10$), i.e., close to the K^+ equilibrium potential as calculated by the Nernst equation ($E_K = -104.1$ mV). *I–V* relationships obtained by plotting currents elicited by N/OFQ at the end of the hyperpolarizing steps against voltage matched those measured by ramp protocols ($n = 5$) (Fig. 1*D*). Varying the external K^+ concentration resulted in a shift of the reversal potential as expected from the Nernst equation with a slope of 54.9 mV per 10-fold change in the external K^+ concentration (Fig. 1*E*) (holding potential −50 mV).

Basic properties of the N/OFQ-induced K^+ current in NRT neurons are summarized in Figure 2. Because responses were not fully reversible, N/OFQ at 1 μM was applied only once in each individual cell, and data from different neurons were pooled. Similar responses to N/OFQ were observed under control conditions (47.6 ± 3.4 pA; $n = 14$) and in the presence of 1 μM TTX (48.2 ± 6.1 pA; $n = 5$), indicating a direct postsynaptic effect of N/OFQ. The effect was significantly reduced in the presence of 100 μM Ba^+ (23.6 ± 2.9 pA; $n = 5$; $p \leq 0.01$). Inclusion of 2 mM GDP-β-*S* as a nonhydrolyzable GDP analog in the pipette solution prevented the induction of an inward rectifier K^+ current by N/OFQ, confirming the involvement of G-proteins ($n = 4$). Application of 3 μM [Nphe^1]nociceptin(1–13)NH_2, an antagonist to the ORL receptor (Calo' et al., 2000a), before addition of 1 μM N/OFQ reduced the N/OFQ response significantly (11.0 ± 4.9 pA; $n = 5$; $p \leq 0.01$). Application of 3 μM [Nphe^1]nociceptin(1–13)NH_2 alone did not change the holding current and thus exerted no agonistic effects ($n = 5$; data not shown). The outward current elicited by N/OFQ was not altered in the presence of the nonselective opioid receptor antagonist naloxone at 10 μM (48.2 ± 3.8 pA; $n = 6$) (Fig. 2). Under the same experimental conditions, naloxone (10 μM) reliably and completely blocked the outward current evoked by the μ-opioid receptor agonist D-Ala^2, *N*-Me-Phe^4, glycinol^5-enkephalin (DAMGO) (2 μM) in neurons of the centrolateral thalamic nucleus ($n = 6$; data not shown).

Properties of the N/OFQ-induced current in VB neurons

In VB neurons, existence of an inward rectifier K^+ current was confirmed in eight of eight tested cells (Fig. 3). Similar to effects

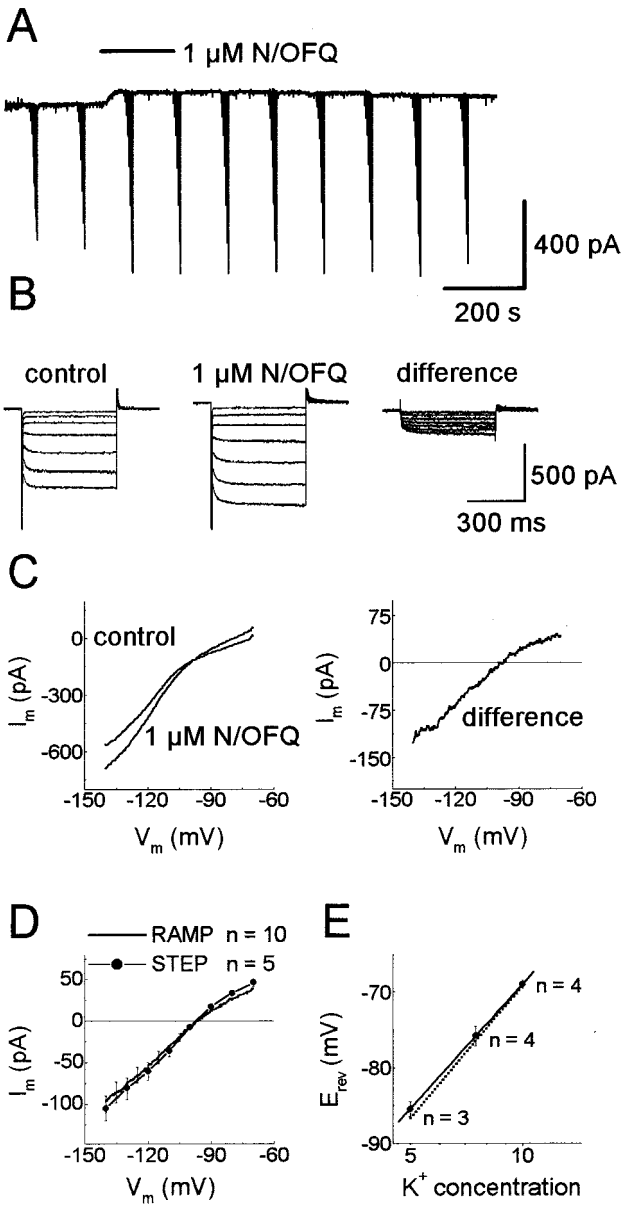

Figure 1. Increase in inwardly rectifying K^+ conductance through N/OFQ in NRT neurons. *A*, Typical response of an NRT neuron to N/OFQ. Under voltage-clamp conditions, application of 1 μM N/OFQ (as indicated above *current trace*) evokes a transient outward current from a holding potential of −70 mV. Downward deflections represent current responses to a voltage-step protocol between −80 and −140 mV as shown on a larger time scale in *B*. Note that the N/OFQ-induced current is associated with an increase in input conductance. *B*, Families of inward currents evoked by hyperpolarizing voltage steps. The difference obtained from recordings before and during action of N/OFQ represents the N/OFQ-induced currents. *C*, *I–V* relationships obtained from voltage ramps (0.2 mV/msec) between −70 and −140 mV. Difference conductance (subtraction of *I–V* relationship during action of N/OFQ from control) displays inward rectification. *D*, Average *I–V* relationships derived by plotting the N/OFQ-induced steady-state current amplitude against voltage (voltage steps as in *A*, *B*) or by using the ramp protocol (protocol as in *C*). Currents reverse near −100 mV, i.e., close to the presumed K^+ equilibrium potential, and display inward rectification. *D*, Shift of reversal potentials of the N/OFQ-evoked current at various external K^+ concentrations according to the Nernst equation (*dotted line*). Data represent averages and SEM obtained from different cells at each concentration (as indicated near error bars) using ramp protocols as in *C*. The *line* was fitted by linear regression.

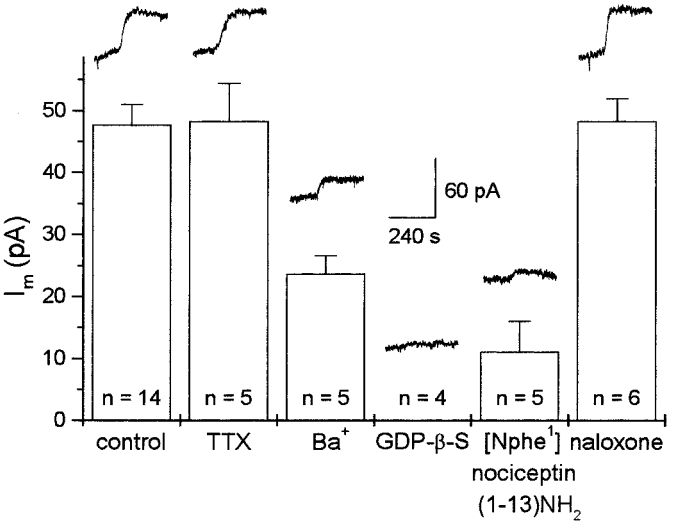

Figure 2. Basic pharmacological properties of the N/OFQ-sensitive current in NRT neurons. N/OFQ responses (1 μM) are similar in amplitude during control conditions and in the presence of 1 μM TTX or 10 μM naloxone, whereas application of external Ba^+ (100 μM) or intracellular GDP-β-*S* (2 mM), or the presence of the ORL antagonist [Nphe^1]nociceptin(1–13)NH_2 (3 μM) leads to a substantial reduction of N/OFQ responses. The *number* of tested cells is indicated at the bottom of the *bars*. *Insets* illustrate typical N/OFQ-induced membrane currents.

on NRT neurons, addition of 1 μM N/OFQ resulted in the activation of an outward current amounting to 33.2 ± 3.5 pA (n = 8) under control conditions that was associated with a decreased membrane resistance (Fig. 3*A*). Ramp protocols as described above (Fig. 3*A*,*B*) revealed an inwardly rectifying current evoked by N/OFQ, which reversed polarity at −97.8 ± 1.0 mV (n = 8) (Fig. 3*C*), i.e., close to the calculated K^+ equilibrium potential (E_K = −104.1 mV).

Lack of effect of N/OFQ on mIPSCs and paired-pulse depression in VB neurons

In view of the major inhibitory input from the NRT to VB neurons, effects of N/OFQ on inhibitory synaptic transmission were analyzed. IPSCs were measured as outward currents using a Cs^+-based internal solution at a holding potential of 0 mV. The induction of K^+ currents by N/OFQ was effectively prevented under these conditions, as was indicated by the lack of change in holding current and membrane conductance after addition of the drug (data not shown). Action potential-evoked transmitter release was blocked by addition of TTX (1 μM) to the bath solution. mIPSCs were pharmacologically isolated in the presence of 10 μM NBQX and 50 μM AP-5 and were completely blocked by the $GABA_A$ receptor antagonist bicuculline (20 μM; n = 4; data not shown). Representative examples before (*top traces*) and after (*bottom traces*) addition of 1 μM N/OFQ are shown in Figure 4, *A* and *B*. The cumulative amplitude and inter-event interval histograms (Fig. 4*B*) were obtained during a period of 60 sec before addition of N/OFQ and after a steady-state had been reached within 2 min after drug application. N/OFQ exerted no effect on amplitude or frequency of mIPSCs in VB neurons (n = 7). Average maximal amplitudes of mIPSC were 26.1 ± 2.2 pA before and 25.9 ± 2.4 pA during the presence of N/OFQ; the frequency of mIPSC amounted to 8.4 ± 1.8 Hz under control conditions and 8.3 ± 1.9 Hz after addition of N/OFQ (n = 7).

Because analysis of miniature synaptic currents may underes-

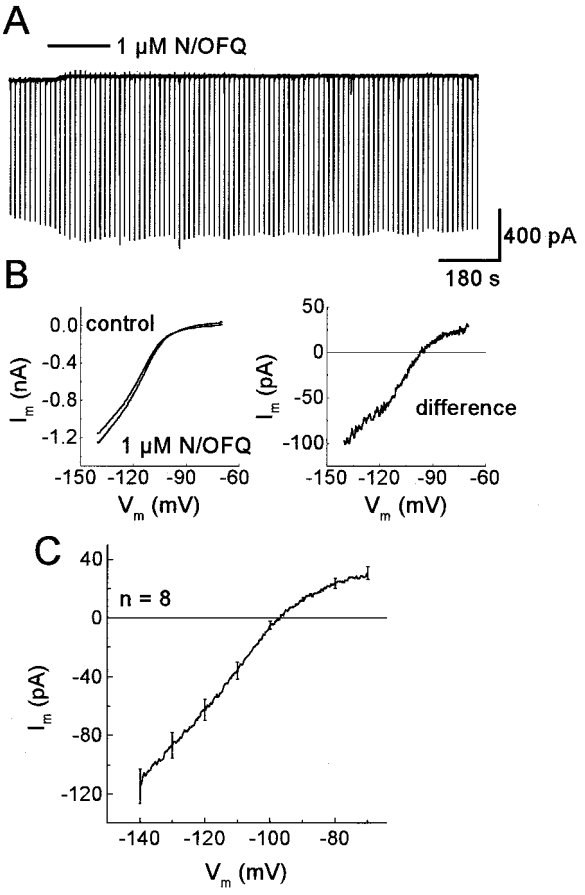

Figure 3. Increase in inwardly rectifying K^+ conductance through N/OFQ in VB neurons. *A*, Typical response of a VB neuron to N/OFQ. Under voltage-clamp conditions, application of 1 μM N/OFQ evokes a transient outward current from a holding potential of −70 mV. Downward deflections represent current responses to voltage ramps from −70 to −140 mV as shown on a larger time scale in *B*. *B*, *I–V* relationships obtained from voltage ramps. The difference obtained from recordings before and during action of N/OFQ represents the N/OFQ-induced current. *C*, Average *I–V* relationships. Current reverses near −100 mV, i.e., close to the presumed K^+ equilibrium potential, and displays inward rectification.

timate influences exerted by N/OFQ through inhibition of voltage-gated Ca^{2+} channels or the activation of G-protein-activated K^+ currents in synaptic terminals, paired-pulse depression of evoked IPSCs was examined. IPSCs evoked in the presence of NBQX and AP-5 were completely blocked by 20 μM bicuculline ($n = 4$; data not shown), indicating mediation by $GABA_A$ receptors. Electrical stimulation within the NRT yielded multipeaked IPSCs in VB neurons (Cox et al., 1997; Leresche et al., 2000), possibly caused by induction of bursts of action potentials in individual NRT cells. Therefore, the stimulating electrode was placed parallel to the borderline of the NRT within the VB, reducing excitation of NRT somata. In three of seven tested cells, amplitudes of IPSCs were significantly ($p \leq 0.05$) reduced to 77.7 ± 4.5% of the control value by application of 1 μM N/OFQ (Fig. 4*C*,*E*), whereas IPSCs in the remaining neurons were unaffected (Fig. 4*D*,*F*). The amplitude of the second IPSC with respect to the amplitude of the first IPSC was 52.9 ± 6.7% ($n = 3$) (Fig. 4*G*) and 58.3 ± 2.8% ($n = 4$) (Fig. 4*H*) in the subpopulations of neurons in which IPSC amplitudes were reduced or unaffected by N/OFQ, respectively. A change in paired-pulse depression ratio after addition of N/OFQ was not observed (Fig. 4*G*,*H*).

Effect of N/OFQ on mEPSCs and paired-pulse facilitation in NRT neurons

To investigate possible effects of N/OFQ on excitatory synaptic input to NRT neurons, mEPSCs were analyzed. Postsynaptic effects of N/OFQ were reliably blocked by inclusion of GDP-β-*S* into the pipette solution, as was confirmed through unaltered holding current and membrane conductance during the course of the experiments (data not shown). $GABA_A$- and NMDA receptor-mediated responses and spike-evoked transmitter release were eliminated through addition of 10 μM bicuculline, 50 μM AP-5, and 1 μM TTX, respectively. Under these conditions, mEPSCs were fully blocked by 10 μM DNQX ($n = 4$; data not shown), indicating mediation by non-NMDA receptors. Typical examples of mEPSCs recorded under control conditions (*top traces*) and in the presence of 1 μM N/OFQ (*bottom traces*) are shown in Figure 5*A*. mEPSCs were analyzed as described previously for mIPSCs (Fig. 5*B*). Mean maximal amplitudes of mEPSCs remained unchanged, amounting to 20.2 ± 1.6 pA in the absence and 19.9 ± 1.5 pA in the presence of N/OFQ ($n = 7$). In three of seven tested cells, the mean frequency of mEPSCs declined significantly ($p \leq 0.05$) from 12.1 ± 1.9 Hz under control conditions to 10.1 ± 1.5 Hz after addition of N/OFQ, reflecting a reduction by 16.3 ± 0.6% ($n = 3$) of the control value. In the remaining cells, no change in mean frequency was observed (control, 11.3 ± 3.4 Hz; N/OFQ, 10.8 ± 3.2 Hz; $n = 4$). Electrical stimulation within the VB elicited EPSCs composed of multiple components in NRT neurons ($n = 4$; data not shown). Therefore, a stimulating electrode was placed parallel to the borderline of the VB within the NRT. Non-NMDA receptor-mediated EPSCs were pharmacologically isolated through the presence of bicuculline (20 μM) and AP-5 (50 μM), as confirmed by the blocking effect of DNQX (10 μM; $n = 5$; data not shown). In five of six cells tested, EPSC amplitudes were significantly ($p \leq 0.05$) reduced to 74.8 ± 6.3% of the control value by application of 1 μM N/OFQ (Fig. 5*C*,*D*). During paired-pulse stimulation, the amplitude of the second relative to that of the first EPSC amounted to 191.8 ± 20.4% before and 217.9 ± 26.1% ($n = 5$) after application of N/OFQ (Fig. 5*E*). Paired-pulse facilitation was not altered in the presence of N/OFQ.

Effects of N/OFQ on spike firing in NRT and VB neurons

Under current-clamp conditions, 1 μM N/OFQ induced a membrane hyperpolarization from the resting membrane potential (NRT, −67.5 ± 1.3 mV, $n = 9$; VB, −68.6 ± 1.0 mV, $n = 9$), with an average maximal amplitude of −6.9 ± 1.0 mV ($n = 9$) in NRT neurons (Fig. 6*A*) and −4.6 ± 0.5 mV ($n = 9$) in VB neurons (Fig. 6*B*). The input membrane resistance decreased from 451.8 ± 64.8 to 341.9 ± 37.5 MΩ (NRT, $n = 9$) and from 382.0 ± 28.1 to 295.3 ± 28.7 MΩ (VB, $n = 9$) during the maximal response, reflecting a reduction to 79.2 ± 4.4% (NRT) and to 76.8 ± 3.9% (VB) of the control value. Typical membrane potential responses to a current step protocol (+0.1 nA) are exemplified in Figure 6, *A* and *B*. Instantaneous frequency plots were constructed from the first four spikes by determining the time elapsed between two consecutive action potentials and plotting the reciprocal value against the spike number in NRT (Fig. 6*C*) and VB neurons (Fig. 6*D*). Instantaneous frequency was significantly (NRT, $p \leq 0.01$; VB, $p \leq 0.05$) increased by addition of 1

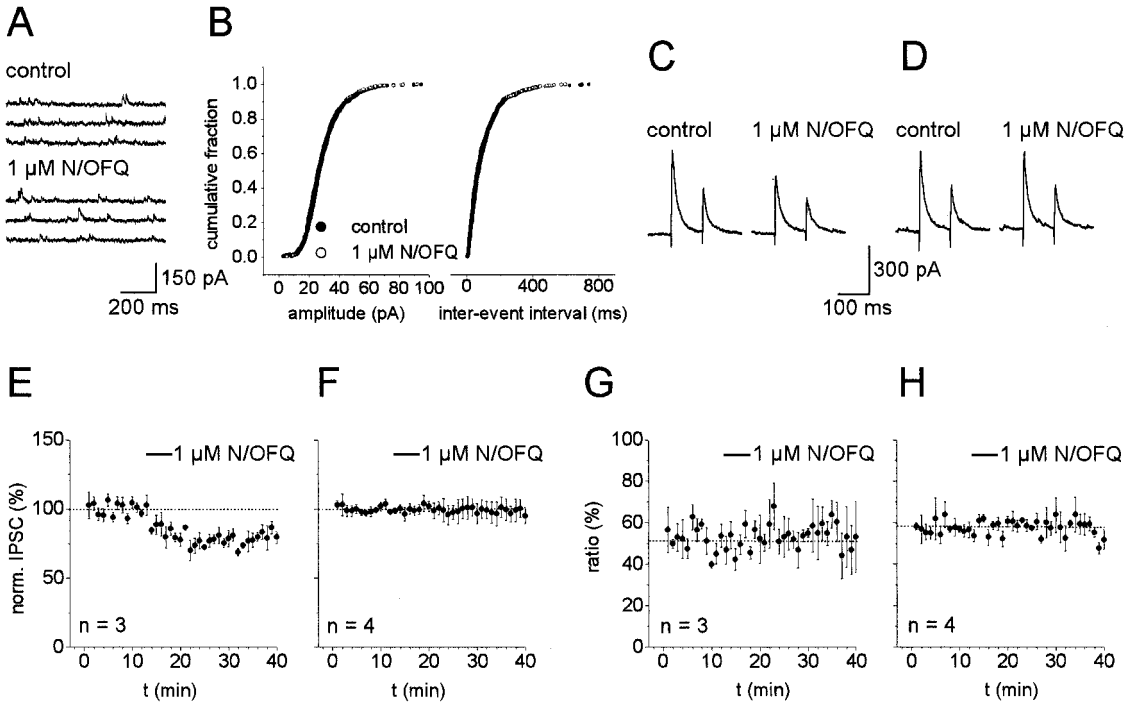

Figure 4. Effects of N/OFQ on inhibitory synaptic transmission in VB neurons. *A*, Examples of mIPSCs recorded in the presence of 1 μM TTX before (*top traces*) and during action of 1 μM N/OFQ (*bottom traces*). *B*, Cumulative amplitude and inter-event interval frequency distributions obtained from the same VB neuron shown in *A* before addition of N/OFQ and after a steady-state effect had been reached. The number of synaptic events counted over time periods of 60 sec amounted to 602 under control conditions and 587 in the presence of N/OFQ. Note that N/OFQ does not affect amplitude or frequency of mIPSCs. *C*, *D*, IPSCs recorded before and after addition of 1 μM N/OFQ. Traces represent averages of three responses to paired stimulation (interstimulus interval 100 msec, repeated at 0.05 Hz) immediately before application of N/OFQ and after a steady-state effect had been reached. In three of seven neurons, IPSC amplitudes were reduced in the presence of the drug (*C*), whereas the remaining cells were unaffected (*D*). *E*, *F*, Time course of the effect of N/OFQ on normalized first IPSC amplitudes. Note the reduction of IPSC amplitude after addition of N/OFQ in a subset of neurons (*E*). *G*, *H*, Lack of N/OFQ effects on paired-pulse depression in the subset of VB neurons in which IPSC amplitudes were reduced (*G*) and unaffected (*H*) by N/OFQ.

μM N/OFQ, indicating a shift from tonic to burst firing mode. Mean spike frequency changed from 36.7 ± 3.3 to 57.8 ± 3.3 Hz (NRT, $n = 6$) and from 30.0 ± 3.3 to 43.3 ± 6.4 Hz (VB, $n = 4$) after addition of N/OFQ.

Under control conditions, hyperpolarizing pulses (−50 pA) applied at resting potential were followed by the activation of a low-threshold calcium spike crowned by one to seven action potentials in four of seven NRT neurons (Fig. 6*E*) and in all tested VB neurons ($n = 9$) (Fig. 6*F*). In the presence of 1 μM N/OFQ, this firing behavior was abolished in all NRT neurons ($n = 7$) (Fig. 6*E*). In VB neurons, six of nine tested cells displayed no rebound spikes after application of 1 μM N/OFQ (Fig. 6*F*). In the remaining VB cells, the average delay time between the end of the hyperpolarizing current step and the generation of the first spike was 111.7 ± 2.4 msec under control conditions and 157.3 ± 14.7 msec in the presence of N/OFQ ($n = 3$). By comparison, N/OFQ had no measurable effect on burst activity evoked by depolarizing current steps from hyperpolarized values of the membrane potential (Fig. 6*G*,*H*). In NRT ($n = 7$) and VB neurons ($n = 9$), the number of spikes in a burst amounted to 6.7 ± 0.7 and 4.4 ± 0.5 in the absence and 7.3 ± 0.7 and 4.4 ± 0.5 in the presence of N/OFQ, respectively. The ratio of spike number generated in the presence and absence of N/OFQ was 1.1 ± 0.04 ($n = 7$) in NRT and 1.0 ± 0.06 ($n = 9$) in VB neurons. Mean spike frequency was 44.8 ± 4.8 Hz (control) and 48.6 ± 4.8 Hz (N/OFQ) in NRT neurons ($n = 7$) and 29.6 ± 3.5 Hz (each condition) in VB neurons ($n = 9$). In addition, instantaneous frequency was unaffected by application of the drug (NRT: 124.9 ± 4.6 Hz, control, 131.0 ± 5.5 Hz, N/OFQ, $n = 7$; VB: 162.3 ± 20.8 Hz, control, 161.4 ± 20.6 Hz, N/OFQ, $n = 7$; first spike interval). Differences were not significant.

Effects of N/OFQ on intrathalamic oscillations

Electrical stimulation of the internal capsule produced oscillatory activity that was detected in extracellular multiple-unit recordings in NRT and VB as described previously (Huguenard and Prince, 1994; Ulrich and Huguenard, 1995). To enhance network oscillation and to reduce the variability between slices, extracellular Mg^{2+} concentration was reduced to 0.8 mM (Cox et al., 1997). Figures 7 and 8 present typical examples of recordings in NRT (Fig. 7*A*) and VB (Fig. 8*A*). In the presence of 1 μM N/OFQ, oscillation was markedly shortened from two up to four cycles compared with eight up to nine cycles under control conditions (Figs. 7*A*, 8*A*). Poststimulus histograms (Figs. 7*B*, 8*B*) were used to quantify onset of rhythmic activity and peak amplitudes reflecting phasic spike discharge. Time to first peak was prolonged significantly by N/OFQ from 401.1 ± 12.5 to 503.3 ± 36.4 msec (NRT, $n = 9$ slices; $p \leq 0.05$) and from 448.8 ± 38.2 to 555.0 ± 42.0 msec (VB, $n = 8$ slices; $p \leq 0.01$). The maximal number of counts during first cycle was reduced significantly from 15.9 ± 2.2 to 5.6 ± 1.8 (NRT, $n = 9$ slices; $p \leq 0.01$) and from 18.3 ± 1.6 to 12.6 ± 1.8 (VB, $n = 8$ slices; $p \leq 0.01$). To assess quantitatively the influence of N/OFQ on duration of rhythmic activity, autocorrelograms of multiple-unit activities (Figs. 7*C*, 8*C*) were con-

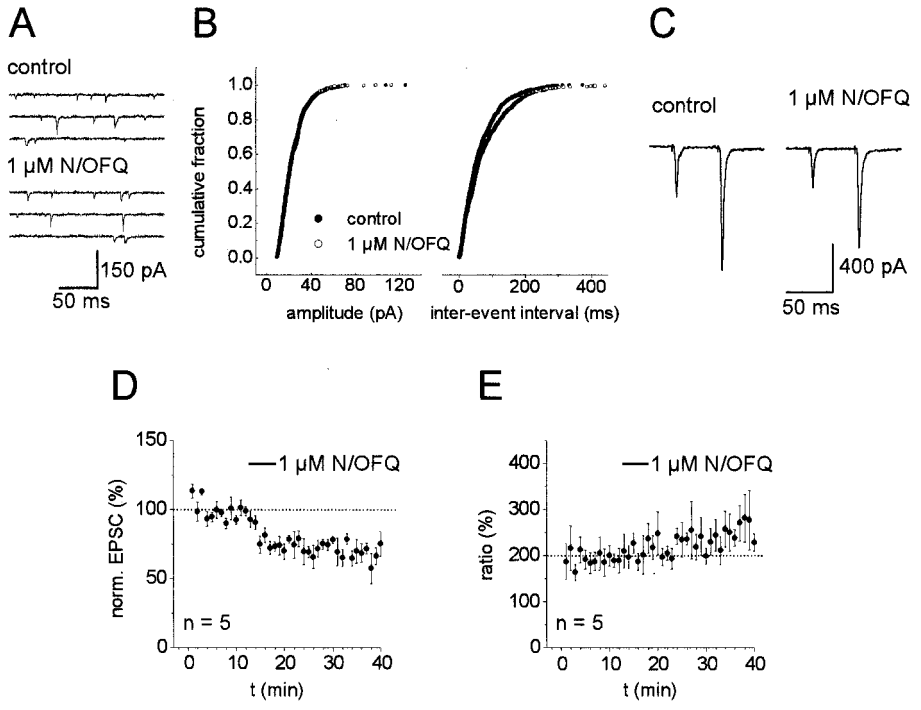

Figure 5. Effects of N/OFQ on excitatory synaptic transmission in NRT neurons. *A*, Examples of mEPSCs recorded in the presence of 1 μM TTX before (*top traces*) and during action of 1 μM N/OFQ (*bottom traces*). *B*, Cumulative amplitude and inter-event interval frequency distributions obtained from the same NRT neuron shown in *A* before addition of N/OFQ and after a steady-state effect had been reached. Note that N/OFQ does not affect the amplitude of mEPSCs but shifts mEPSC inter-event intervals to larger values in three of seven neurons. The number of synaptic events counted over time periods of 60 sec amounted to 937 under control conditions and 775 in the presence of N/OFQ. *C*, EPSCs recorded before and after addition of 1 μM N/OFQ. Traces represent averages of three responses elicited at 0.05 Hz obtained immediately before application of N/OFQ and after a steady-state effect had been reached. In five of six neurons, EPSC amplitudes were reduced in the presence of the drug. *D*, Time course of the effect of N/OFQ on normalized first EPSC amplitudes. Note the reduction of EPSC amplitude after addition of N/OFQ. *E*, Time course of paired-pulse facilitation during application of N/OFQ. Note that the paired-pulse ratio is unchanged by N/OFQ.

structed. Duration was shortened significantly by N/OFQ from 4.3 ± 0.3 to 1.8 ± 0.4 sec in NRT ($n = 9$ slices; $p \leq 0.01$) and from 5.3 ± 0.9 to 2.9 ± 0.9 sec in VB ($n = 8$ slices; $p \leq 0.05$). The mean oscillation frequency remained unchanged in the presence of N/OFQ, amounting to 3.8 ± 0.1 and 3.7 ± 0.2 Hz in NRT ($n = 9$ slices) and to 3.2 ± 0.2 Hz ($n = 8$ slices) and 3.1 ± 0.4 Hz ($n = 6$ slices) in VB.

DISCUSSION

Postsynaptic effects induced by N/OFQ

The present results demonstrate an inhibitory action of N/OFQ on postsynaptic cell excitability in NRT and VB neurons. N/OFQ induced an increase in an inwardly rectifying K^+ conductance in every recorded neuron, as was indicated by the *I–V* relationship of responses to N/OFQ, their sensitivity to low concentrations of extracellular Ba^{2+}, and their dependence on extracellular K^+. In the presence of intracellular GDP-β-*S*, a nonhydrolyzable GDP analog (Gilman, 1987), N/OFQ effects were prevented, confirming the involvement of G-proteins. The N/OFQ-evoked outward current was significantly reduced by [Nphe^1]nociceptin(1–13)NH_2, an antagonist to the ORL receptor (Calo' et al., 2000a). Naloxone, a prototypical antagonist to the μ-, δ-, and κ-subtypes of opioid receptors (Raynor et al., 1994), had no effect on N/OFQ responses but blocked DAMGO-evoked outward currents in centrolateral thalamic neurons under the same experimental conditions. Furthermore, OP2 receptors, known to bind [Nphe^1]nociceptin(1–13)NH_2 with some affinity (Calo' et al., 2000a), do not seem to exist in NRT and VB (Mansour et al., 1987, 1994). Therefore it seems reasonable to conclude that responses to N/OFQ were mediated through ORL receptors. The increase of an inwardly rectifying potassium conductance was very similar in NRT and VB neurons and resembled those described in other systems (Henderson and McKnight, 1997; Meunier, 1997; Darland et al., 1998; Meis and Pape, 1998; Caló et al., 2000b). Besides activating a K^+ conductance, N/OFQ has been shown to modulate various voltage-dependent Ca^{2+} currents (Calo' et al., 2000b), including the T-type current (Abdulla and Smith, 1997). Although the effects of N/OFQ on isolated Ca^{2+} currents were not studied in NRT and VB neurons, N/OFQ elicited no measurable effect on calcium-mediated burst activity evoked by depolarizing steps from hyperpolarized values of the membrane potential, arguing against a substantial inhibition of T-type Ca^{2+} currents in this preparation.

N/OFQ effects on synaptic transmission

Thalamocortical VB neurons and NRT neurons are mutually interconnected through an extensive axonal network, with thalamocortical axon collaterals forming excitatory synaptic connections with NRT neurons and NRT axons contacting VB neurons in a feedback manner (for review, see Steriade et al., 1997). In the rat VB, GABAergic interneurons are rarely encountered (Harris and Hendrickson, 1987), and no local axon collaterals were detected (Harris, 1987). Therefore it seems feasible to conclude that the axonal connections between the NRT and the VB are a major source of the postsynaptic currents recorded in the present study. It is fair to add, however, that a possible contribution particularly to spontaneous synaptic currents of additional inputs, such as those originating in the cortex or brainstem, cannot be excluded.

During experiments focusing on synaptic interactions in the present study, postsynaptic actions of N/OFQ in the individual neuron under study were reliably blocked through the use of a Cs^+-based internal solution or inclusion of GDP-β-*S* into the pipette solution, as was validated by unaltered holding current, membrane conductance, and mIPSC or mEPSC amplitudes after addition of N/OFQ.

Inhibitory synaptic transmission in VB neurons is not affected by N/OFQ through a direct modulation of axonal release as was indicated by the following lines of evidence. mIPSC frequency in VB neurons was unchanged after addition of the peptide. Miniature postsynaptic currents are usually thought to result from the spontaneous exocytosis of transmitter-containing vesicles occur-

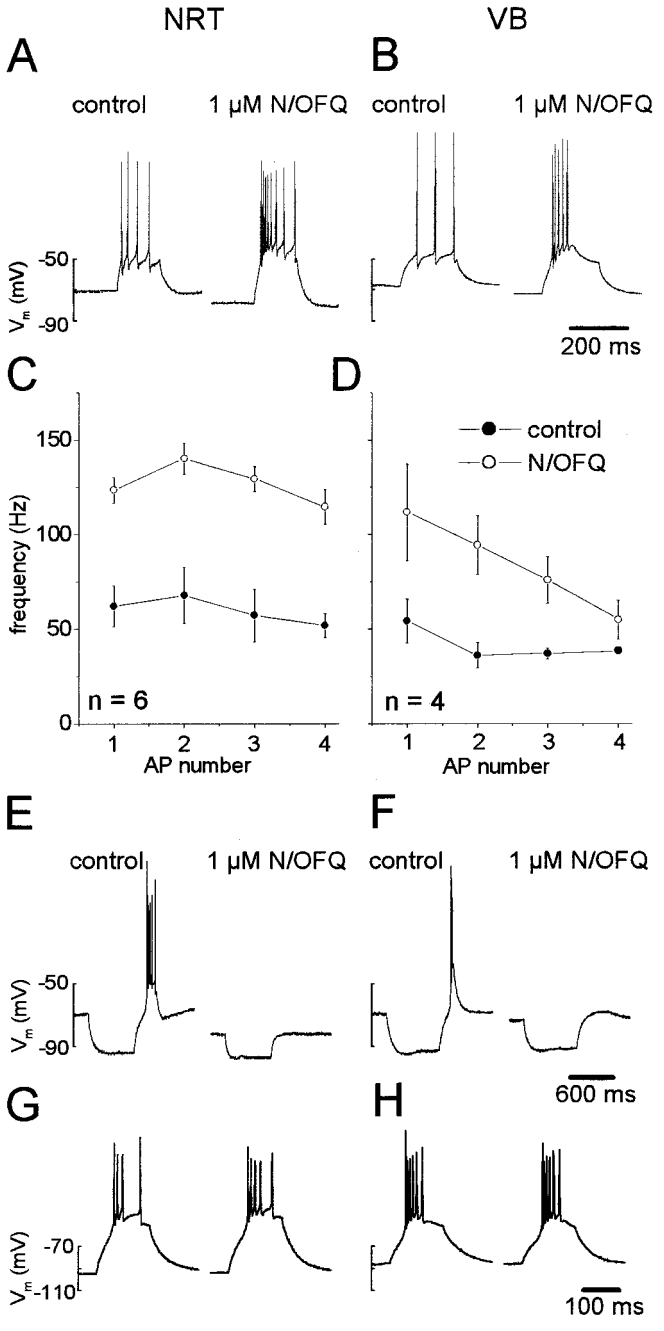

Figure 6. Firing behavior of NRT and VB neurons during action of N/OFQ under current-clamp conditions. *A*, *B*, Application of 1 μM N/OFQ induces a hyperpolarizing response in NRT (*A*) as well as VB (*B*) neurons, favoring the shift from tonic to bursting firing mode (current step + 100 pA). *C*, *D*, Instantaneous frequency is significantly increased by addition of 1 μM N/OFQ. Plots are constructed from the first four spikes by determining the time elapsed between two consecutive action potentials and plotting the reciprocal value against the spike number in NRT (*C*) or VB neurons (*D*). *E*, *F*, Hyperpolarizing pulses (−50 pA) applied at resting potential are followed by the activation of a low-threshold calcium spike crowned by several action potentials. Rebound bursts are reduced in the presence of N/OFQ in NRT (*E*) as well as VB (*F*) neurons. *G*, *H*, Depolarizing pulses (+100 pA, NRT; +120 pA, VB) applied at hyperpolarized membrane potentials provoke bursting firing mode in the presence or absence of N/OFQ in NRT (*G*) as well as VB (*H*) neurons.

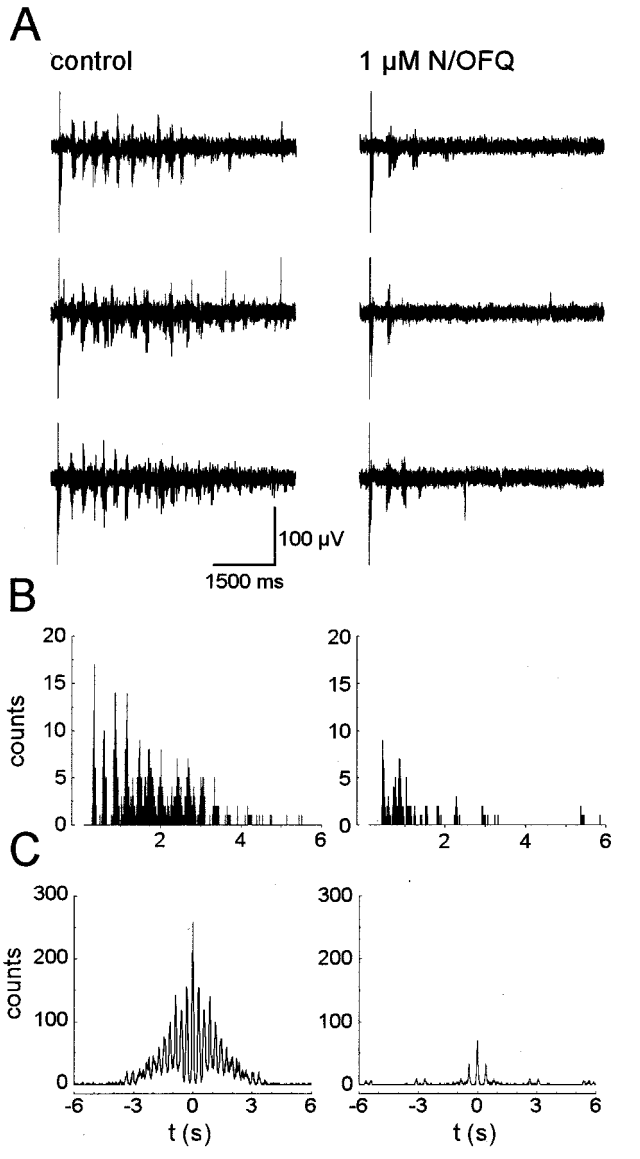

Figure 7. Depression of intrathalamic rhythms by N/OFQ in NRT neurons. *A*, Consecutive extracellular multiunit recordings in control solution and after addition of 1 μM N/OFQ. Stimulation of the internal capsule evokes several cycles of rhythmic discharge that are attenuated by addition of N/OFQ. *B*, Onset of rhythmic activity and peak amplitudes reflecting phasic spike discharge are prolonged or reduced, respectively, in the presence of N/OFQ as assessed by poststimulus histograms. *C*, Autocorrelograms of multiunit activities show the substantial decrease in duration of rhythmic activity induced by N/OFQ.

ring in the absence of Ca^{2+} influx (Miller, 1998). As a result, analysis of mPSCs may underestimate mechanisms of inhibition upstream of Ca^{2+} entry, namely inhibition of Ca^{2+} channels or activation of K^+ channels within the nerve terminal. Therefore, the amplitude ratio of paired stimuli was analyzed. Release probability in response to a second stimulus given in rapid succession to a first one depends on presynaptic processes, resulting in paired-pulse depression or facilitation (Davies et al., 1993; Thomson, 2000; Waldeck et al., 2000). N/OFQ did not affect paired-pulse depression of IPSCs in VB neurons, further arguing against the modulation of presynaptic mechanisms involving receptors localized on relevant terminals. On the other hand, the amplitudes of evoked IPSCs were reduced. The most likely

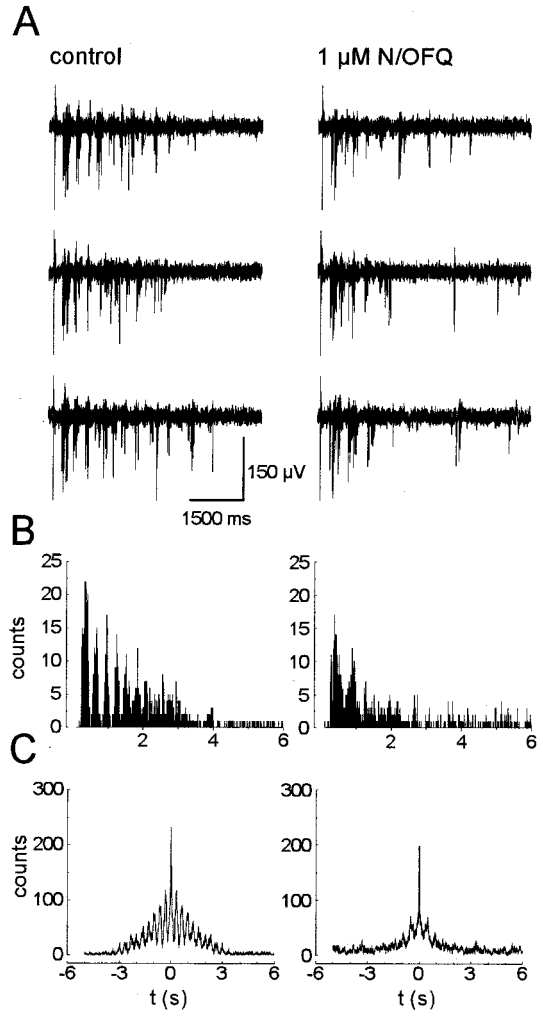

Figure 8. Depression of intrathalamic rhythms by N/OFQ in VB neurons. *A*, Consecutive extracellular multiunit recordings in control solution and after addition of 1 μM N/OFQ. Stimulation of the internal capsule evokes several cycles of rhythmic discharge, which are attenuated by addition of N/OFQ. *B*, Onset of rhythmic activity and peak amplitudes reflecting phasic spike discharge are prolonged or reduced, respectively, in the presence of N/OFQ as assessed by poststimulus histograms. *C*, Autocorrelograms of multiunit activities show the substantial decrease in duration of rhythmic activity induced by N/OFQ.

explanation is that the stimulating electrode, besides activating axon collaterals of NRT neurons, in addition activated the somatodendritic membrane of nearby NRT neurons attributable to the immediate vicinity of VB and NRT. The activation of K^+ channels located in the somatodendritic membrane of presynaptic NRT neurons by N/OFQ would then lead to reduced spike activity, associated with a reduction of transmitter release.

In the NRT, excitatory synaptic transmission is modulated only to a minor extent, if at all, through presynaptic mechanisms of N/OFQ. A subtle change of mEPSC frequency was detected in the presence of N/OFQ in a subpopulation of recorded neurons, whereas differences in paired-pulse facilitation after addition of N/OFQ were not observed. The stimulating electrode was placed between NRT and VB to activate predominantly axon collaterals originating in the VB. Therefore, the effect of N/OFQ on mEPSCs may relate to additional glutamatergic inputs not activated during paired-pulse recordings. The depression of evoked EPSCs in the NRT most likely results from the inhibition of presynaptic VB neurons.

The overall conclusion from these data is that N/OFQ reduces intrathalamic synaptic transmission predominantly through activation of K^+ channels located in the somatodendritic membrane of NRT and VB neurons rather than through a synaptic site of action.

Functional significance of N/OFQ effects in the thalamus

Firing properties of thalamic neurons include tonic firing of fast Na^+/K^+-mediated action potentials and rhythmic bursting triggered by a low-threshold Ca^{2+} spike (Steriade et al., 1993; McCormick and Bal, 1997). Generation of rhythmic activities is supported by the reciprocal interaction of excitatory thalamic relay neurons with GABAergic NRT neurons in conjunction with these intrinsic membrane properties of the involved neuronal population (McCormick, 1992). Burst discharges of NRT neurons evoke IPSCs in thalamocortical relay neurons, which in turn generate rebound Ca^{2+} spikes crowned by fast action potentials reexciting NRT neurons (Steriade et al., 1997).

The increase of an inwardly rectifying potassium conductance in the postsynaptic membrane of NRT and VB neurons by N/OFQ promoted a significant hyperpolarization of membrane potential, thereby inhibiting tonic firing and favoring a shift toward burst mode. On the other hand, the associated decrease in membrane input resistance effectively reduced the generation of burst firing after relief of membrane hyperpolarization. It is important to add that burst firing evoked through depolarizing current steps from a hyperpolarized value of the membrane potential was unaltered after addition of N/OFQ, thereby arguing against an effect of the peptide on the mediating Ca^{2+} channels (see above). The hyperpolarization-activated cation current I_h involved in the generation of rhythmic activity is not expressed in NRT neurons (Santoro et al., 2000) and was unaltered by application of N/OFQ in VB neurons (data not shown). Furthermore, as is discussed above, N/OFQ has very little if any direct effect on inhibitory and excitatory synaptic transmission in the NRT/VB network. From these findings it seems feasible to conclude that the N/OFQ-evoked dampening of intrathalamic oscillations mainly relates to the activation of an inwardly rectifying K^+ conductance in both NRT and VB neurons. In the presence of N/OFQ, intrathalamic rhythms showed delayed onset, reduced amplitude, and shortened duration. Reduced excitability of NRT neurons would result in reduced inhibitory drive onto VB neurons. After a reduction of rebound burst output from VB, NRT neurons would receive less re-excitation. This cycle would substantially dampen rhythmic activity. The cellular mechanisms of actions of N/OFQ differ from those of other peptides studied in the thalamus, such as somatostatin or neuropeptide Y (NPY). Somatostatin had no effect on postsynaptic membrane properties of VB neurons but reduced mIPSC frequency in 22% of encountered cells by 37% (Leresche et al., 2000). NPY was demonstrated to downregulate GABA release in terminals of NRT and VB neurons by inhibition of Ca^{2+} influx via NPY_2 receptors (Sun et al., 2001a). In addition, a G-protein-dependent inwardly rectifying K^+ conductance was activated through NPY_1 receptors, reducing directly neuronal excitability, thereby resembling the action of N/OFQ (Sun et al., 2001b). Effects of these neuropeptides on thalamic oscillations were not assessed in these studies. The neuropeptide cholecystokinin (CCK) reportedly decreased a leak K^+ conductance resulting in a long-lasting membrane depo-

larization in NRT neurons but exerted no direct effects on VB neurons (Cox et al., 1995). CCK had dual effects on intrathalamic rhythms. Low concentrations suppressed or prolonged oscillations, whereas higher concentrations exerted predominantly anti-oscillatory effects. The latter were attributed to the change in firing mode in NRT neurons from burst to single spike, resulting in decreased inhibitory current and reduced probability of burst output from VB neurons (Cox et al., 1997).

Although the possible sources of N/OFQ in thalamus are well documented, the mechanisms that mediate the release of N/OFQ and action of a transmitter are not. Low to moderate signals for the ORL receptor are evenly distributed in thalamic nuclei (Shimohira et al., 1997; Sim and Childers, 1997; Ikeda et al., 1998; Neal et al., 1999a; Letchworth et al., 2000), suggesting that N/OFQ may act as a transmitter inherent to the intrathalamic circuitry. Despite numerous efforts, including electrical stimulation within the thalamus at different sites using different stimulation protocols, a response sensitive to selective ORL antagonists could not be reliably obtained in the present study (data not shown). On the other hand, signal intensity for messenger RNA encoding the precursor prepro-N/OFQ is highest in the NRT, which, in addition, shows intense immunohistochemical staining of the peptide (Ikeda et al., 1998; Neal et al., 1999b). This anatomical evidence points to an endogenous role of N/OFQ within the thalamic network. In support of this were the findings that N/OFQ evoked a postsynaptic response in all recorded NRT neurons in the present study.

Finally, it is interesting to note that opioid receptor activation was associated with an increase in postsynaptic K^+ conductance, similar to that observed with N/OFQ, in the thalamus. Opioidergic inhibition via μ-opioid receptors was prevalent among relay neurons in different areas and in ~50% of NRT neurons (Brunton and Charpak, 1997, 1998). By comparison, all VB or NRT neurons showed a K^+-mediated inhibition after application of N/OFQ (this study). In various systems, ORL and classical opioid receptors share common cellular actions but have distinct pharmacological profiles and behavioral effects related to pain modulation (Darland et al., 1998; Yamamoto et al., 1999; Brundege, 2000). One issue is whether N/OFQ produces analgesia or hyperalgesia, which may relate to opposing actions on distinct groups of neurons, particularly in pain-modulating circuits (Heinricher et al., 1997; Pan et al., 2000). The dampening effect of N/OFQ on intrathalamic oscillations votes in favor of a pain-modulatory influence also on the thalamic level, although the consequences on the systems and behavioral level remain to be evaluated.

REFERENCES

Abdulla FA, Smith PA (1997) Nociceptin inhibits T-type Ca^{2+} channel current in rat sensory neurons by a G-protein-independent mechanism. J Neurosci 17:8721–8728.

Barlocco D, Cignarella G, Giardina GA, Toma L (2000) The opioid-receptor-like 1 (ORL-1) as a potential target for new analgesics. Eur J Med Chem 35:275–282.

Benoist JM, Kayser V, Gacel G, Zajac JM, Gautron M, Roques B, Guilbaud G (1986) Differential depressive action of two μ and δ opioid ligands on neuronal responses to noxious stimuli in the thalamic ventrobasal complex of rat. Brain Res 398:49–56.

Brundege JM (2000) Orphanin FQ/nociceptin and the mystery of pain. Neuron 26:282–285.

Brunton J, Charpak S (1997) Heterogeneity of cell firing properties and opioid sensitivity in the thalamic reticular nucleus. Neuroscience 78:303–307.

Brunton J, Charpak S (1998) μ-Opioid peptides inhibit thalamic neurons. J Neurosci 18:1671–1678.

Calo' G, Guerrini R, Bigoni R, Rizzi A, Marzola G, Okawa H, Bianchi C, Lambert DG, Salvadori S, Regoli D (2000a) Characterization of [Nphe^1]nociceptin(1–13)NH_2, a new selective nociceptin receptor antagonist. Br J Pharmacol 129:1183–1193.

Calo' G, Guerrini R, Rizzi A, Salvadori S, Regoli D (2000b) Pharmacology of nociceptin and its receptor: a novel therapeutic target. Br J Pharmacol 129:1261–1283.

Cox CL, Huguenard JR, Prince DA (1995) Cholecystokinin depolarizes rat thalamic reticular neurons by suppressing a K^+ conductance. J Neurophysiol 74:990–1000.

Cox CL, Huguenard JR, Prince DA (1997) Peptidergic modulation of intrathalamic circuit activity *in vitro*: actions of cholecystokinin. J Neurosci 17:70–82.

Darland T, Heinricher MM, Grandy DK (1998) Orphanin FQ/nociceptin: a role in pain and analgesia, but so much more. Trends Neurosci 21:215–221.

Davies CH, Pozza MF, Collingridge GL (1993) CGP 55845A: a potent antagonist of GABAB receptors in the CA1 region of rat hippocampus. Neuropharmacology 32:1071–1073.

Gilman AG (1987) G proteins: transducers of receptor-generated signals. Annu Rev Biochem 56:615–649.

Grisel JE, Mogil JS (2000) Effects of supraspinal orphanin FQ/nociceptin. Peptides 21:1037–1045.

Harris RM (1987) Axon collaterals in the thalamic reticular nucleus from thalamocortical neurons of the rat ventrobasal thalamus. J Comp Neurol 258:397–406.

Harris RM, Hendrickson AE (1987) Local circuit neurons in the rat ventrobasal thalamus: a GABA immunocytochemical study. Neuroscience 21:229–236.

Harrison LM, Grandy DK (2000) Opiate modulating properties of nociceptin/orphanin FQ. Peptides 21:151–172.

Hawes BE, Graziano MP, Lambert DG (2000) Cellular actions of nociceptin: transduction mechanisms. Peptides 21:961–967.

Heinricher MM, McGaraughty S, Grandy DK (1997) Circuitry underlying antiopioid actions of orphanin FQ in the rostral ventromedial medulla. J Neurophysiol 78:3351–3358.

Henderson G, McKnight AT (1997) The orphan opioid receptor and its endogenous ligand—nociceptin/orphanin FQ. Trends Pharmacol Sci 18:293–301.

Huguenard JR, Prince DA (1994) Intrathalamic rhythmicity studied *in vitro*: nominal T-current modulation causes robust anti-oscillatory effects. J Neurosci 14:5485–5502.

Ikeda K, Watanabe M, Ichikawa T, Kobayashi T, Yano R, Kumanishi T (1998) Distribution of prepro-nociceptin/orphanin FQ mRNA and its receptor mRNA in developing and adult mouse central nervous systems. J Comp Neurol 399:139–151.

Leresche N, Asprodini E, Emri Z, Cope DW, Crunelli V (2000) Somatostatin inhibits GABAergic transmission in the sensory thalamus via presynaptic receptors. Neuroscience 98:513–522.

Letchworth SR, Mathis JP, Rossi GC, Bodnar RJ, Pasternak GW (2000) Autoradiographic localization of ^{125}I[Tyr^{14}]orphanin FQ/nociceptin and ^{125}I[Tyr^{10}]orphanin FQ/nociceptin(1–11) binding sites in rat brain. J Comp Neurol 423:319–329.

Mansour A, Khachaturian H, Lewis ME, Akil H, Watson SJ (1987) Autoradiographic differentiation of mu, delta, and kappa opioid receptors in the rat forebrain and midbrain. J Neurosci 7:2445–2464.

Mansour A, Fox CA, Meng F, Akil H, Watson SJ (1994) κ_1 receptor mRNA distribution in the rat CNS: comparison to κ receptor binding and prodynorphin mRNA. Mol Cell Neurosci 5:124–144.

McCormick DA (1992) Neurotransmitter actions in the thalamus and cerebral cortex and their role in neuromodulation of thalamocortical activity. Prog Neurobiol 39:337–388.

McCormick DA, Bal T (1997) Sleep and arousal: thalamocortical mechanisms. Annu Rev Neurosci 20:185–215.

Meis S, Pape HC (1998) Postsynaptic mechanisms underlying responsiveness of amygdaloid neurons to nociceptin/orphanin FQ. J Neurosci 18:8133–8144.

Meis S, Pape HC (2001) Control of glutamate and GABA release by nociceptin/orphanin FQ in the rat lateral amygdala. J Physiol (Lond) 532:701–712.

Meunier J-C (1997) Nociceptin/orphanin FQ and the opioid receptor-like ORL1 receptor. Eur J Pharmacol 340:1–15.

Meunier J-C, Mollereau C, Toll L, Suaudeau C, Moisand C, Alvinerie P, Butour J-L, Guillemot J-C, Ferrara P, Monsarrat B, Mazarguil H, Vassart G, Parmentier M, Costentin J (1995) Isolation and structure of the endogenous agonist of opioid receptor-like ORL_1 receptor. Nature 377:532–535.

Millan MJ (1999) The induction of pain: an integrative review. Prog Neurobiol 57:1–164.

Miller RJ (1998) Presynaptic receptors. Annu Rev Pharmacol Toxicol 38:201–227.

Moran TD, Abdulla FA, Smith PA (2000) Cellular neurophysiological actions of nociceptin/orphanin FQ. Peptides 21:969–976.

Neal Jr CR, Mansour A, Reinscheid R, Nothacker HP, Civelli O, Akil H, Watson Jr SJ (1999a) Opioid receptor-like (ORL1) receptor distribution in the rat central nervous system: comparison of ORL1 receptor

mRNA expression with ^{125}I-[^{14}Tyr]-orphanin FQ binding. J Comp Neurol 412:563–605.
Neal Jr CR, Mansour A, Reinscheid R, Nothacker HP, Civelli O, Watson Jr SJ (1999b) Localization of orphanin FQ (nociceptin) peptide and messenger RNA in the central nervous system of the rat. J Comp Neurol 406:503–547.
Neher E (1992) Correction for liquid junction potentials in patch clamp experiments. Methods Enzymol 207:123–131.
Pan Z, Hirakawa N, Fields HL (2000) A cellular mechanism for the bidirectional pain-modulating actions of orphanin FQ/nociceptin. Neuron 26:515–522.
Raynor K, Kong H, Chen Y, Yasuda K, Yu L, Bell GI, Reisine T (1994) Pharmacological characterization of the cloned κ-, δ-, and μ-opioid receptors. Mol Pharmacol 45:330–334.
Reinscheid RK, Nothacker H-P, Bourson A, Ardati A, Henningsen RA, Bunzow JR, Grandy DK, Langen H, Monsma FJ, Civelli O (1995) Orphanin FQ: a neuropeptide that activates an opioid like G protein-coupled receptor. Science 270:792–794.
Santoro B, Chen S, Luthi A, Pavlidis P, Shumyatsky GP, Tibbs GR, Siegelbaum SA (2000) Molecular and functional heterogeneity of hyperpolarization-activated pacemaker channels in the mouse CNS. J Neurosci 20:5264–5275.
Schlicker E, Morari M (2000) Nociceptin/orphanin FQ, neurotransmitter release in the central nervous system. Peptides 21:1023–1029.
Shigenaga Y, Inoki R (1976) Effect of morphine on single unit responses in ventrobasal complex (VB) and posterior nuclear group (PO) following tooth pulp stimulation. Brain Res 103:152–156.
Shimohira I, Tokuyama S, Himeno A, Niwa M, Ueda H (1997) Characterization of nociceptin-stimulated in situ [^{35}S]GTPγS binding in comparison with opioid agonist-stimulated ones in brain regions of the mice. Neurosci Lett 237:113–116.
Sim LJ, Childers SR (1997) Anatomical distribution of mu, delta, and kappa opioid- and nociceptin/orphanin FQ-stimulated [^{35}S]guanylyl-5′-O-(γ-thio)-triphosphate binding in guinea pig brain. J Comp Neurol 386:562–572.
Standifer KM, Pasternak GW (1997) G proteins and opioid receptor-mediated signalling. Cell Signal 9:237–248.
Steriade M, McCormick DA, Sejnowski TJ (1993) Thalamocortical oscillations in the sleeping and aroused brain. Science 262:679–685.
Steriade M, Jones EG, McCormick DA (1997) The thalamus: organisation and function. New York: Elsevier.
Sun QQ, Akk G, Huguenard JR, Prince DA (2001a) Differential regulation of GABA release and neuronal excitability mediated by neuropeptide Y_1 and Y_2 receptors in rat thalamic neurons. J Physiol (Lond) 531:81–94.
Sun QQ, Huguenard JR, Prince DA (2001b) Neuropeptide Y receptors differentially modulate G-protein-activated inwardly rectifying K^+ channels, high-voltage-activated Ca^{2+} channels in rat thalamic neurons. J Physiol (Lond) 531:67–79.
Thomson AM (2000) Facilitation, augmentation, potentiation at central synapses. Trends Neurosci 23:305–312.
Ulrich D, Huguenard JR (1995) Purinergic inhibition of GABA and glutamate release in the thalamus: implications for thalamic network activity. Neuron 15:909–918.
Waldeck RF, Pereda A, Faber DS (2000) Properties and plasticity of paired-pulse depression at a central synapse. J Neurosci 20:5312–5320.
Xu X, Grass S, Hao J, Xu IS, Wiesenfeld-Hallin Z (2000) Nociceptin/orphanin FQ in spinal nociceptive mechanisms under normal, pathological conditions. Peptides 21:1031–1036.
Yamamoto T, Nozaki-Taguchi N, Sakashita Y, Kimura S (1999) Nociceptin/orphanin FQ: role in nociceptive information processing. Prog Neurobiol 57:527–535.